

Coupling between two collinear air-core Bragg fibers.

M. Skorobogatiy^a, Kunimasa Saitoh and Masanori Koshiba^b,

^a École Polytechnique de Montréal, Génie physique,
C.P. 6079, succ. Centre-Ville Montréal, QC, Canada H3C 3A7;

^bDivision of Media and Network Technologies, Hokkaido University,
Sapporo 060-0814, Japan

ABSTRACT

We characterize coupling between two identical collinear hollow core Bragg fibers, assuming TE_{01} launching condition. Using multipole method and finite element method we investigate dependence of the beat length between supermodes of the coupled fibers and supermode radiation losses as a function of the inter-fiber separation, fiber core radius and index of the cladding. We established that coupling is maximal when fibers are touching each other decreasing dramatically during the first tens of nanometers of separation. However, residual coupling with the strength proportional to the fiber radiation loss is very long range decreasing as an inverse square root of the inter-fiber separation, and exhibiting periodic variation with inter-fiber separation. Finally, coupling between the TE_{01} modes is considered in a view of designing a directional coupler. We find that for fibers with large enough core radii one can identify broad frequency ranges where inter-modal coupling strength exceeds super-mode radiation losses by an order of magnitude, thus opening a possibility of building a directional coupler. We attribute such unusually strong inter-mode coupling both to the resonant effects in the inter-mirror cavity as well as a proximity interaction between the leaky modes localized in the mirror.

1. INTRODUCTION

Recently, hollow core Photonic Band Gap (PBG) microstructured and Bragg fibers have been experimentally demonstrated to exhibit guidance and low transmission loss at $1.55\mu\text{m}$,¹ $3.0\mu\text{m}$ and $10.6\mu\text{m}$ ² promising considerable impact in the long haul and high power guidance applications almost anywhere in the IR. Hollow PBG fibers are able to guide light through the hollow (gaseous) core featuring very low material loss and nonlinearity, and achieving radiation confinement via reflection from the surrounding high quality dielectric multilayer mirror. Development of such fibers motivated the interest in design of directional couplers

based on the PBG fibers to provide a uniform guiding/switching fabric, where the same type of fiber is used to guide and to manipulate light.

Because of the wider availability of microstructured PBG fibers, most of the recent experimental and theoretical work has concentrated on the design of directional couples based on such fibers.³⁻⁷ Particularly, on the preform stage, silica rods are arranged to form two closely spaced silica or air cores separated by several air-silica layers, all surrounded by a hexagonal lattice of silica rods. When preform is drawn the resultant microstructured fiber exhibits two closely spaced identical cores surrounded by a photonic crystal reflector. Coupling between such cores is characterized by finite element or finite difference methods with integrated absorbing boundary conditions.⁸⁻¹¹

In this work we for the first time, to our knowledge, consider the coupling between another type of PBG fibers - hollow Bragg fibers. Our main interest is to characterize coupling strength between collinear PBG Bragg fibers, and propagation losses of the lowest loss "telecommunication quality"¹² TE_{01} -like supermodes. The issue of inter-fiber modal coupling can be of importance when several hollow photonic crystal fibers are placed in the proximity of each other, because of the established in this work a very long radiation driven interaction range between such fibers. We also address the possibility of building Bragg fiber based directional couplers for TE_{01} modes. Unlike for PBG microstructured fibers, the current process of Bragg fiber fabrication does not allow placing the cores of two Bragg fibers arbitrarily close, while creating a common PBG reflector on the outside of both cores. We show that enhanced resonant coupling is still possible even with standard Bragg fibers by tuning the separation between them to specific values with Bragg fiber mirrors of adjacent fibers creating an open resonant cavity.

The outline of our paper is as follows. We start by justifying most of the coupling properties between collinear PBG Bragg fibers based on the analogy with 1D Bragg gratings with defects. We then characterize the inter-fiber coupling as a function of core separation and index of the cladding. Finally, we discuss the

Send e-mail to: maksim.skorobogatiy@polymtl.ca

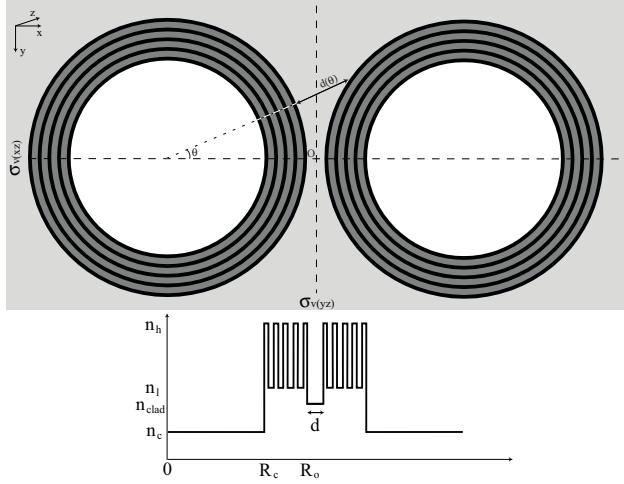


Figure 1. Schematics of the two identical collinear hollow Bragg fibers separated by the inter-mirror distance d . Dielectric profile along the inter-fiber center line resembles a 1D Bragg grating with a central defect corresponding to the inter-mirror cavity.

possibility of building directional coupler based on the resonant interaction between the fibers.

2. ANALOGY TO THE 1D BRAGG GRATING WITH DEFECTS

We consider two collinear hollow PBG Bragg fibers of core radius R_c , outer mirror radius R_o and inter-mirror separation d . On Fig. 1 we present schematics of the system together with a dielectric profile along the line passing through the fiber centers. We assume that the PBG mirror is made of two dielectrics with refractive indexes $n_h > n_l > n_c$, where n_c is a core index (for hollow fibers $n_c = 1$), while corresponding mirror layer thicknesses d_h, d_l are chosen to form a quarter-wave stack for the grazing angles of incidence.¹² Thus, denoting λ to be the center wavelength of the primary Band Gap, then $d_h \sqrt{n_h^2 - n_c^2} = d_l \sqrt{n_l^2 - n_c^2} = \lambda/4$. Cladding index n_{clad} can be chosen at will.

By inspection of Fig. 1, dielectric profile along the fiber center line resembles a 1D Bragg grating made of the fiber reflector mirrors and a central defect of size d corresponding to the inter-mirror cavity. Quarter-wave thickness of each mirror layer ensures the largest Band Gap (stop band) of the reflector Bragg grating, so that radiation incoming from the hollow core onto the containing mirror will be maximally reflected. However, when optical length of the central defect in the Bragg grating is $\lambda\nu/2$, $\nu \in (0, 1, \dots)$ it is known that transmission trough such a grating will exhibit a narrow maximum at λ , although transmission everywhere else in

the Bragg grating stop band will be still strongly suppressed. In the case of two identical Bragg fibers, the first resonance happens when the fibers are touching $d = 0$ as the two outside high index layers of the fiber-mirrors create a $\lambda/2$ defect (see Fig. 1). Introducing a free space wave number $k = 2\pi/\lambda$, modal propagation constant β , and transverse modal wave number in the defect layer of refractive index n and thickness d as $k_n^t = \sqrt{(kn)^2 - \beta^2}$, we rewrite resonant condition for a half-wavelength defect as $dk_n^t = \pi\nu$. Thus, anytime the inter-mirror separation d approaches its resonant value we expect increase in the inter-fiber coupling due to enhanced radiation leakage from one core to another mediated by the resonant inter-mirrors cavity. Spectral width and the maximum of an enhanced coupling peak will be a strong function of the inter-mirror cavity Q factor. Because of the cylindrical shape of the fiber Bragg reflectors, inter-mirror cavity Q factor is ultimately limited by the fiber finite curvature $\sim R_o^{-1}$. Finally, to increase the spectral width of a coupling peak one can adopt a standard solution from the theory of flattened passband filters¹⁵ where the structure of the Bragg reflector is modified to present a sequence of several low quality $\lambda/4$ stacks coupled together by $\lambda/2$ defects, exhibiting a designable spectral width step-like transmission response.

We now address the impact of cladding index n_{clad} on the PBG Bragg fiber coupling. It was established in,¹² that low loss modes in the PBG Bragg fibers have their propagation constants situated closely to the core material light line, particularly for TE_{01} mode, $1 - \beta/(kn_c) \sim (\lambda/R_c)^2$. Typical values of the core radii for a long-haul PBG Bragg fiber¹² being $R_c \sim 10 - 15\lambda$. Thus, in the core material $k_{n_c}^t = \sqrt{(kn_c)^2 - \beta^2} \sim R_c^{-1}$, while in the material with $n > n_c$, $k_n^t \simeq k\sqrt{n^2 - n_c^2}$. Thus, if cladding index is the same as the core index $n_{clad} = n_c$, one expects resonant increase in the coupling between PBG Bragg fibers at $d = \pi\nu/(k_{n_c}) \sim \nu R_c$, while if $n_{clad} > n_c$, then $d \simeq \lambda\nu/(2\sqrt{n_{clad}^2 - n_c^2})$ where in both cases $\nu \in (0, 1, \dots)$.

Finally, as the distance $L = 2R_o + d$ between the fiber centers increase, intensities of the radiated fields from the core of one fiber at the position of the second fiber will decrease with distance as $E \sim \sqrt{Im(\beta)/L}$, where $Im(\beta)$ is proportional to the modal radiation loss (from the energy conservation argument). Classical consideration of inter-fiber coupling between similar modes suggests that coupling strength is proportional to the overlap of the fields of one fiber in the mirror region of another fiber, leading to the $Im(\beta)/\sqrt{L}$ dependence of the PBG Bragg fiber coupling strength with the modal loss and inter-fiber separation.

3. COUPLING AS A FUNCTION OF INTER-FIBER SEPARATION

We analyze coupling between the the lowest loss “telecommunication quality” TE_{01} modes of the two collinear PBG Bragg fibers employing a modified multipole method.^{13,14} In a stand along fiber, TE_{01} is a singlet, with zero electric field components along the direction of propagation and radial direction¹² (electric field vector is circling parallel to the dielectric interfaces). When second identical fiber is introduced, rotational symmetry of a single fiber is broken and interaction between the TE_{01} modes of the Bragg fibers leads to appearance of the two supermodes with propagation constants β^- and β^+ close to β . Remaining symmetry of a system is described by $C2v$ group that includes reflections in (XZ) , (YZ) planes and inversion with respect to the system symmetry center O (see Fig. 1). Symmetry considerations result in the following symmetries of the transverse electric field components of supermodes: supermode⁻ $E_x(x, -y) = -E_x(x, y)$, $E_y(x, -y) = E_y(x, y)$, $E_x(-x, y) = E_x(x, y)$, $E_y(-x, y) = -E_y(x, y)$, and supermode⁺ $E_x(x, -y) = -E_x(x, y)$, $E_y(x, -y) = E_y(x, y)$, $E_x(-x, y) = -E_x(x, y)$, $E_y(-x, y) = E_y(x, y)$. Thus, at the system symmetry center O , supermode⁺ will have a local maximum of the electric field, while supermode⁻ will have a node.

We first quantify coupling strength between fibers and radiation losses of the supermodes as a function of the inter-mirror separation d for the case when $n_c = n_{clad}$. We characterize inter-fiber coupling strength by the difference in the real parts of supermode propagation constants $\delta\beta = |\beta^+ - \beta^-|$, while modal radiation losses are defined by the imaginary parts of their propagation constants. Bragg fiber under study has 7 mirror layers (starting and ending with a high index layer), $n_c = 1$, $n_h = 2.8$, $n_l = 1.5$, $n_{clad} = n_c = 1$, $R_c = 5\mu m$, operating wavelength is $1.55\mu m$. On Fig. 2 normalized coupling strength and radiation losses of supermodes are presented. Normalization factor is radiation loss of a TE_{01} mode, which for this fiber is $11.2dB/m$. Such a normalization choice allows us to largely decouple the structure of the reflector from other geometrical variables such as inter-fiber separation. One observes that coupling strength exhibits periodical variation as separation between fibers increase. Locations of the maxima in coupling strength match well with the predicted half wave condition for the optical defect length $d = \pi\nu/(k_{n_c}) \sim \nu R_c$ (marked by the vertical dotted lines). Locations of the maxima in supermode losses are also close to the half-wave separation between fiber mirrors, suggesting that loss increase is due to field leakage

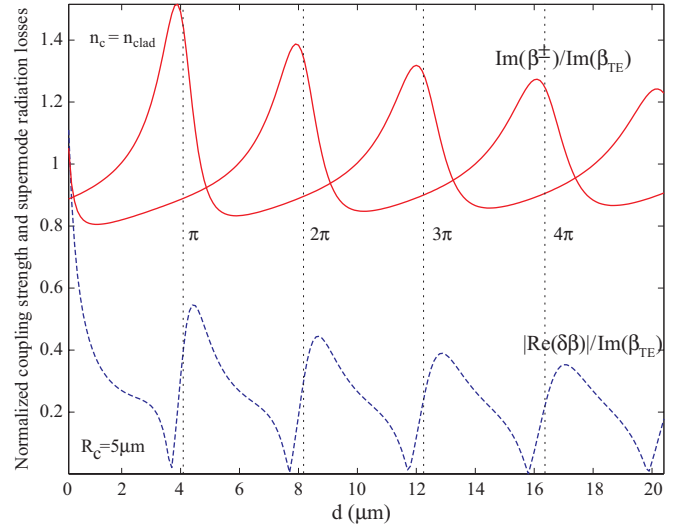


Figure 2. Normalized coupling strength $|Re(\delta\beta)|/Im(\beta_{TE})$ and supermode radiation losses $Im(\beta^+)/Im(\beta_{TE})$, $Im(\beta^-)/Im(\beta_{TE})$ in a system of two collinear hollow Bragg fibers as a function of inter-mirror separation d . Cladding index is the same as core index $n_c = n_{clad}$. All the curves are normalized by the radiation losses of the TE_{01} mode of a stand alone hollow Bragg fiber.

out of the open inter-mirror cavity, where at resonance field intensity is enhanced. From Fig. 2 one also observes a very slow decrease in coupling with inter-fiber separation. By analyzing the values of the coupling maxima as a function of distance up to $d = 100\mu m$ a clear $|\delta\beta| \sim (2R_o + d)^{-0.5}$ dependence is observed.

As argued in the previous section, when $n_c = n_{clad}$ position of the maxima of modal coupling scales proportionally to the core radius R_c . On Fig. 3 we verify this scaling by plotting normalized coupling and supermode radiation losses as a function of the inter-fiber separation for three Bragg fibers having different core radii and the same dielectric profile as before. Predicted scaling is clearly observable from the plot. When comparing the values of the modal coupling at the first maxima, one observes that the coupling slowly increases as the fiber core radius increases. When looking in the region of small inter-mirror separations $0.2\mu m < d < 1\mu m$ (left subplot of Fig. 3) one observes a substantial increase in the coupling strength that considerably surpasses the supermode radiation losses when the distance between mirrors is decreased. Moreover, for the same inter-mirror separation d , the coupling strength increases with an increase in the fiber core radius, signifying that the quality of the inter-mirror cavity resonator increases as R_c increases.

Overall, from Figs. 2, 3 we observe that coupling be-

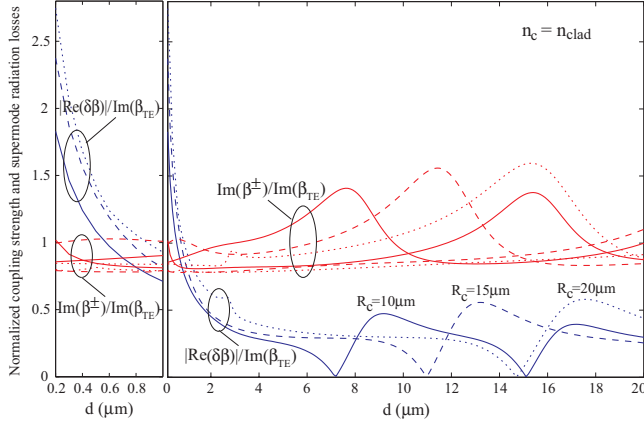


Figure 3. Normalized coupling strength and supermode radiation losses of coupled hollow Bragg fibers as a function of inter-mirror fiber separation d . Cladding index is the same as core index $n_c = n_{clad}$. Different line types correspond to Bragg fibers of different core radii, solid lines - $R_c = 10\mu m$, dashed lines - $R_c = 15\mu m$, and dotted lines - $R_c = 20\mu m$. Left plot is a blow-up of the region where fibers nearly touch $0.2\mu m < d < 1\mu m$ showing dramatic increase in the fiber coupling compared to almost constant radiation losses of the supermodes.

tween Bragg fibers stays comparable to the supermode radiation losses even at very large separations, while in the region of almost touching fibers $d < 1\mu m$ coupling strength considerably exceeds supermode radiation losses. Thus, supermode beat length $\pi/|\delta\beta|$ (characteristic length of the fiber link after which considerable amount of power in one fiber gets transferred into another fiber) remains smaller or comparable to the supermode decay length $1/Im(\beta^\pm)$ even for large inter-fiber separations $d \sim 100\mu m$. Hence, extra care should be taken to absorb the radiation fields of the leaky modes when dealing with closely spaced Bragg fibers.

Next, we investigate coupling strength between fibers and supermode radiation losses as a function of inter-mirror separation d when $n_{clad} > n_c$. Bragg fibers under study have the same dielectric profile and operating wavelength as before except for the value of the cladding index $n_{clad} = 1.3$. On Fig. 4 we present the normalized coupling strength and supermode radiation losses for three different Bragg fibers of core radii $R_c = 5\mu m$, $R_c = 10\mu m$ and $R_c = 20\mu m$ as a function of the inter-mirror separation around their second maximum. By inspection of Fig. 4 we observe that independently of the fiber core radius, locations of the second maxima $\nu = 1$ in the coupling strength match well with the predicted based on the half-wave condition for the

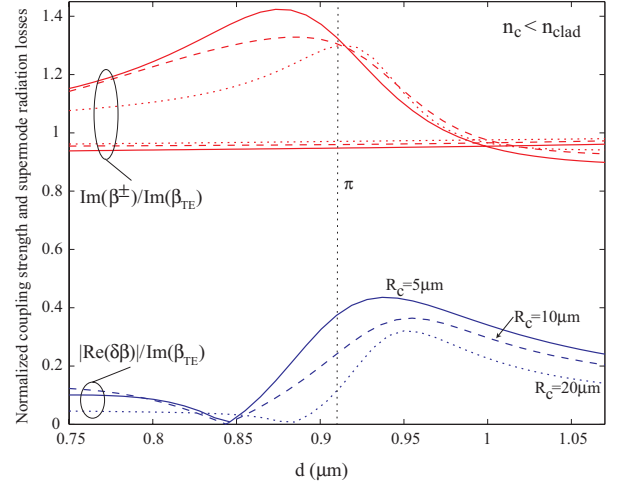


Figure 4. Normalized coupling strength and supermode radiation losses of coupled hollow Bragg fibers as a function of inter-mirror fiber separation d around second resonance. Cladding index is larger than core index $n_{clad} = 1.3$, $n_c = 1$. Different line types correspond to different Bragg fiber core radii, solid lines - $R_c = 5\mu m$, dashed lines - $R_c = 10\mu m$, and dotted lines - $R_c = 20\mu m$. Maximum of the coupling strength slowly decreases as fiber core radius increases.

optical defect length $d = \lambda\nu/(2\sqrt{n_{clad}^2 - n_c^2})$ (marked by the dotted line). When comparing the values of the fiber coupling at the first maxima, one observes that the coupling slowly decreases as the fiber core radius increases.

Difference in behavior of the inter-fiber coupling strength with the change of fiber core radius R_c for the cases $n_c = n_{clad}$ and $n_{clad} > n_c$ can be rationalized as following. Resonant phenomena in the inter-mirror cavity comes from a coherent addition of the multiply reflected radial waves originally radiated from the fiber core. Phase difference that radial wave experiences by traversing from the first mirror to the second depends strongly on the inter-mirror separation. In turn, inter mirror separation depends on the angle θ (see Fig. 1) at which the wave escapes the core. For small angles and $d \ll R_o$, $d(\theta) \simeq d(0) + R_o\theta^2$. Phase shift that radial wave experience after one trip is $\phi(\theta) = d(\theta)k_n^t$, where k_n^t is a transverse wave number. Thus, waves travelling at different angles will have somewhat different phases, and at some critical θ_c the phase difference $\phi(\theta_c) - \phi(0) = \pi$ will lead to destructive interference of waves in the inter-mirror cavity. The larger the θ_c the higher the quality of the resonator will be. When $n_c = n_{clad}$, $\phi(\theta) - \phi(0) = R_o\theta^2 k_{n_c}$, and as $k_{n_c} \sim R_c^{-1}$, $R_c \sim R_o$ we arrive at $\theta_c \sim 1$ which is independent of the core radius. In contrast, when $n_{clad} > n_c$,

$\phi(\theta) - \phi(0) = R_o \theta^2 k_n$, and as $k_n \simeq \omega \sqrt{n^2 - n_c^2}$, then $\theta_c \sim \sqrt{\lambda/R_c}$, thus slowly decreasing as the core radius increases. Hence, in the case $n_{clad} > n_c$ the quality of the resonator decreases when the core radius is increased.

Finally, we have also observed that the multipole method¹³ while performing very efficiently at the inter-mirror separations $d/R_o > 0.1$, exhibits slow convergence at smaller separations, and at $d/R_o < 0.01$ convergence becomes problematic. To further study touching fibers we resort to a finite element mode solver with absorbing boundary conditions.

4. COUPLING BETWEEN TOUCHING BRAGG FIBERS

In this section we study feasibility of designing a directional coupler based on two touching hollow Bragg fibers studied by the finite element mode solver.⁸ In the following we assume the same structure of the two Bragg fibers as before, now touching along their length ($d = 0$ in Fig.1), designed for $1.55\mu m$ operation wavelength with index of the cladding matched with that of a core $n_{clad} = n_c = 1$. We first characterize coupling strength between fibers and radiation losses of the supermodes as a function of the fiber core radii R_c at a fixed frequency of $\lambda = 1.45\mu m$. Because of the cylindrical shape of the fiber Bragg reflectors, inter-mirror cavity Q factor is limited by the mirror finite curvature, with Q and, thus, inter-fiber coupling increasing for larger core radii.

In Fig. 5 normalized coupling strength and radiation losses of supermodes are presented. Normalization factor for each curve is a corresponding radiation loss of TE_{01} mode of a stand alone fiber. One observes that with increasing core radius coupling strength exhibits a tendency of gradual increase relative to the radiation losses of the supermodes. For the core radii larger than $10\mu m$ the ratio of the coupling strength to supermode radiation loss approaches a factor of 10 allowing, in principle, to build a directional coupler. Resonant features correspond to the points of accidental degeneracy of TE_{01} with higher order modes.

In Fig. 6 we plot normalized coupling strength and supermode radiation losses as a function of wavelength λ for $R_c = 15\mu m$ and three different inter-fiber separations $d = 0\mu m$, $d = 0.2\mu m$ and $d = 0.5\mu m$. For $d = 0.5\mu m$ the coupling strength is weak and on the order of the supermode radiation losses, changing smoothly as a function of frequency. As inter-fiber separation decreases, the coupling strength exhibits a rapid increase across a broad frequency range together with

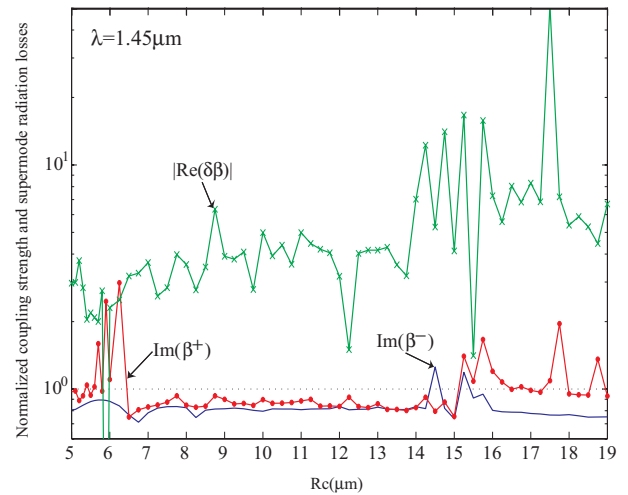


Figure 5. Normalized coupling strength and supermode radiation losses as a function of fiber core radii R_c at $\lambda = 1.45\mu m$. With increasing core radius one observes a tendency of gradual increase of the coupling strength relative to the highest radiation loss of the supermodes.

appearance of many sharp resonances ($d = 0.2\mu m$ in Fig. 6). When fibers are touching $d = 0\mu m$ the coupling strength strongly dominates supermode radiation losses in a broad frequency range. For $1.4\mu m < \lambda < 1.55\mu m$, for example, the ratio of coupling strength to the supermode radiation losses reaches a factor of 10. For a corresponding planar system of grating-defect-grating with a dielectric profile of Fig. 1 the resonance peak is, however, only several nanometers wide which is in contradiction with the Fig. 6 very broad resonant features. Thus, a simple picture of enhanced inter-fiber coupling has to be modified. As spectral width of the enhanced coupling peak depends strongly on the inter-mirror cavity Q factor, we believe that broad resonant features in Fig. 6 can be explained by low Q factor of the resonant inter-mirror cavity due to a finite curvature of the fiber. As our mode solver was limited to the core radii less than $20\mu m$ we were not able to investigate further the narrowing of the resonance for larger radii. Another prominent feature of Fig. 6 is a presence of sharp and broad regions of increase in the supermode losses. Because of a multimoded nature of hollow Bragg fibers, lowest loss TE_{01} mode exhibits multiple points of accidental degeneracies with higher loss modes. At such degeneracy points TE_{01} -like supermode exhibits sharp loss increase by “picking-up” some of the higher order mode loss. In general, we find that broad frequency regions of increase in the supermode losses are due to interaction with low angular momenta modes. For example, by inspecting band diagram of a stand alone

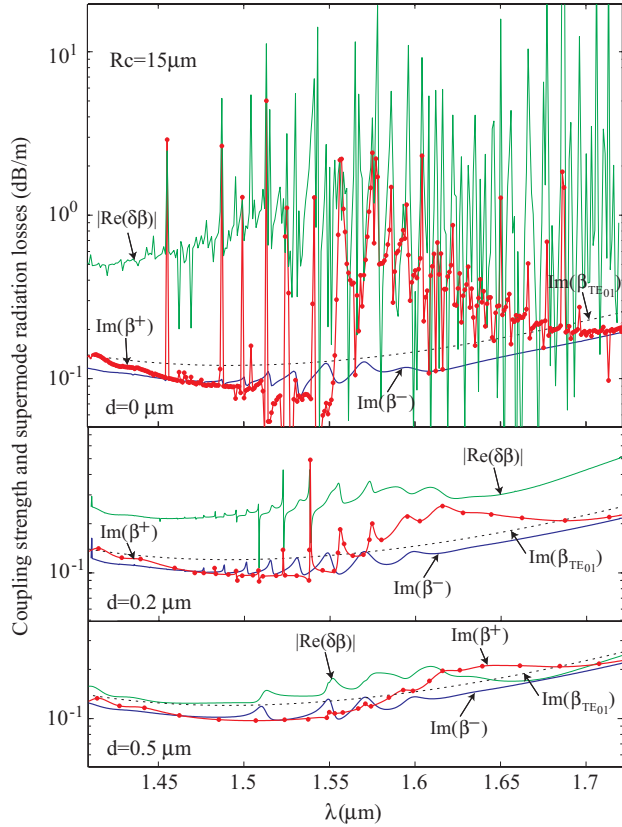


Figure 6. Normalized coupling strength and supermode radiation losses as a function of wavelength λ for $R_c = 15\mu\text{m}$ and inter-fiber separations $d = 0, 0.2, 0.5\mu\text{m}$. For $1.4\mu\text{m} < \lambda < 1.55\mu\text{m}$ one observes a factor of 10 ratio of coupling strength to the highest radiation loss of the supermodes. Sharp resonances in the coupling strength correspond to the accidental mode crossing of TE_{01} with high angular momenta modes of the reflector. In the insert $d = 0\mu\text{m}$, the $|Ey|$ fields are presented at the frequencies close and directly at one of the sharp resonances. The region of $1.55\mu\text{m} < \lambda < 1.65\mu\text{m}$ is dominated by a prolong coupling between TE_{01} and an $m = 2$ mode leading to a broad resonance and an increase in the supermode losses.

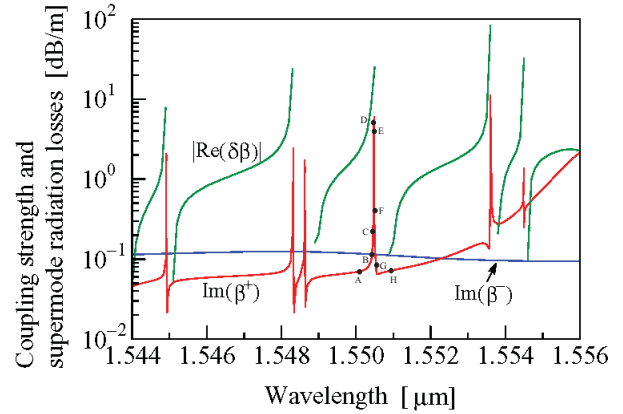


Figure 7. Sharp resonances around the points of degeneracies of a TE_{01} mode with the high angular momentum mirror modes. A, B, C, D, E, F, G, H are the points around one of such resonances at $1.5504\mu\text{m}$.

fiber we find that in the region $1.55\mu\text{m} < \lambda < 1.65\mu\text{m}$ an $m = 2$ mode crosses TE_{01} mode twice staying almost degenerate with it in the whole interval. In Fig. 6, $d = 0\mu\text{m}$ this broad modal interaction region is characterized by an increase in a supermode loss. We have further verified our assumption by modifying the location of the modal degeneracy region by adding more layers to the reflector, and observed a consistent shift of a broad resonance.

On the other hand, by inspecting the modal fields around the sharp resonances (Figs. 7, 8) we conclude that such resonances correspond to the points of degeneracies of a TE_{01} mode with the high angular momentum mirror modes. Note that Fig. 7 is the same as Fig. 6, $d = 0$ but calculated with higher resolution around just a few sharp resonances. At resonance, a hybrid mode has intensity maximum in the inter-mirror cavity defect while the fields in the hollow fiber cores are reduced. We have verified that in a stand alone fiber there is a large number of high angular momenta $m > 6$ leaky modes with propagation constants close to the air line and fields concentrated mostly in the fiber reflector. In a region just outside of the fiber such modes exhibit a fast decay in the cladding. Thus, sharp resonances due to interaction with such modes disappear quickly with increase in the inter-fiber separation as clearly observable in Fig. 6 $d = 0, 0.2, 0.5\mu\text{m}$.

5. DISCUSSION

To summarize, we found that unlike in silica fibers, where the modal tail decays exponentially into the

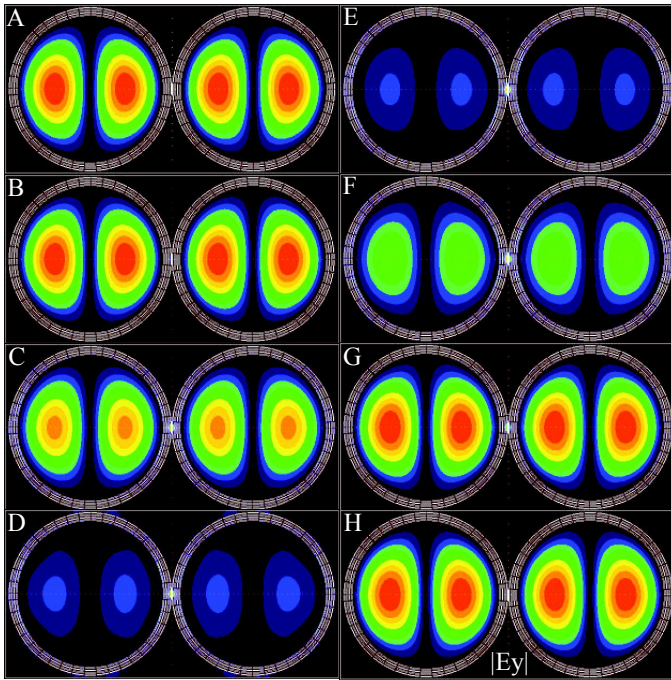


Figure 8. Amplitude of the modal field component $|E_y|$ at the points A,B,C,D,E,F,G,H of Fig. 7 around one of the sharp resonances (black is zero). Points D and E correspond to the excited mirror-cavity modes.

cladding, the radiation field from a hollow PBG Bragg fiber decays in the cladding very slowly as an inverse of the square root of the inter-fiber separation exhibiting periodic oscillations. Moreover, the beat length between supermodes $\pi/Re(\beta^+ - \beta^-)$ stays on the order of the supermode decay length $1/Im(\beta^\pm)$ even for very large inter-fiber separations $\sim 100\mu m$. When two straight pieces of PBG Bragg fiber are spaced less than $1\mu m$ from each other we observed a dramatic increase in the modal coupling without a substantial increase in the supermode losses. We demonstrated that for two touching PBG Bragg fibers of substantially large core radius the frequency regions can be identified where a large increase in the modal coupling is observed without a substantial increase in the supermode losses. In this regime, the supermode beat length becomes much smaller than the supermode decay length, opening a possibility of building a directional coupler exhibiting only a fraction of modal losses along the coupler length. Because of the multimoded nature of hollow PBG Bragg fibers, special care should be taken to avoid accidental modal degeneracies between the mode of operation and higher order modes at the frequency of interest.

REFERENCES

1. C.M. Smith, N. Venkataraman, M.T. Gallagher, D. Muller, J.A. West, N.F. Borrelli, D.C. Allan, K.W. Koch, "Low-loss hollow-core silica/air photonic bandgap fibre," *Nature* **424**, 657-659 (2003).
2. B. Temelkuran B, S.D. Hart, G. Benoit, J.D. Joannopoulos, Y. Fink, "Wavelength-scalable hollow optical fibres with large photonic bandgaps for CO2 laser transmission," *Nature* **420**, 650-653 (2002).
3. M.A. van Eijkelenborg, A. Argyros, G. Barton, I.M. Bassett, M. Fellew, G. Henry, N.A. Issa, M.C.J. Large, S. Manos, W. Padden, L. Poladian, J. Zargari, "Recent progress in microstructured polymer optical fibre fabrication and characterisation," *Opt. Fiber Techn.* **9**, 199-209 (2003).
4. B.H. Lee, J.B. Eom, J. Kim, D.S. Moon, U.-C. Paek, and G.-H. Yang, "Photonic crystal fiber coupler," *Opt. Lett.* **27**, 812-814 (2002).
5. G. Kakarantzas, B.J. Mangan, T.A. Birks, J.C. Knight, P.S.J. Russell, "Directional coupling in a twin core photonic crystal fiber using heat treatment," *Technical Digest. Summaries, Conference on Lasers and Electro-Optics*, 599-600 (2001).
6. M. Kristensen, "Mode-coupling in photonic crystal fibers with multiple cores," *Conf. Digest. CLEO Europe*, 1 (2000).
7. B.J. Mangan, J.C. Knight, T.A. Birks, P.St.J. Russell, and A.H. Greenaway, "Experimental study of dualcore photonic crystal fibre," *Electron. Lett.* **36**, 1358-1359 (2000).
8. K. Saitoh, Y. Sato, and M. Koshiba, "Coupling characteristics of dual-core photonic crystal fiber couplers," *Opt. Express* **11**, 3188-3195 (2003), <http://www.opticsexpress.org/abstract.cfm?URI=OPEX-11-24-3188>.
9. L. Zhang and C. Yang, "Polarization splitter based on photonic crystal fibers," *Opt. Express* **11**, 1015-1020 (2003), <http://www.opticsexpress.org/abstract.cfm?URI=OPEX-11-9-1015>
10. K. Saitoh and M. Koshiba, "Full-vectorial imaginary-distance beam propagation method based on a finite element scheme: application to photonic crystal fibers," *IEEE J. Quantum Electron.* **38**, 927-933 (2002).
11. F. Fogli, L. Saccomandi, P. Bassi, G. Belanca, and S. Trillo, "Full vectorial BPM modeling of indexguiding photonic crystal fibers and couplers," *Opt. Express* **10**, 54-59 (2002), <http://www.opticsexpress.org/abstract.cfm?URI=OPEX-10-1-54>

12. Steven G. Johnson, Mihai Ibanescu, M. Skorobogatiy, Ori Weisberg, Torkel D. Engeness, Marin Soljačić, Steven A. Jacobs, J. D. Joannopoulos, and Yoel Fink, "Low-loss asymptotically single-mode propagation in large-core OmniGuide fibers," *Optics Express* **9**, 748 (2001).
13. T. P. White, B. T. Kuhlmeiy, R. C. McPhedran, D. Maystre, G.C. Martijn de Sterke, and L. C. Botten, "Multipole method for microstructured optical fibers. I. Formulation," *J. Opt. Soc. Am. B* **19**, 2322 (2002).
14. M. Skorobogatiy, K. Saitoh, and M. Koshiba, "Coupling between two collinear air-core Bragg fibers," *J. Opt. Soc. Am. B* **21**, 2095 (2004).
15. R.A. Minasian, K.E. Alameh, E.H.W. Chan, "Photonics-based interference mitigation filters," *IEEE Transactions on Microwave Theory and Techniques* **49**, 1894 (2001)
16. P. Yeh, A. Yariv, and E. Marom, "Theory of Bragg fiber," *J. Opt. Soc. Am.* **68**, 1196–1201 (1978).